Steel and Composite Structures, *Vol. 30, No. 5 (2019) 443-456*
DOI: https://doi.org/10.12989/scs.2019.30.5.443

Cyclic behaviour of infilled steel frames with different beam-to-column connection types

Mohammed A. Sakr [a], Mohammed M. Eladly[*], Tarek Khalifa [b] and Saher El-Khoriby [c]

Department of Structural Engineering, Faculty of Engineering, Tanta University, Tanta, Egypt

(*Received September 22, 2018, Revised February 23, 2019, Accepted March 5, 2019*)

Abstract. Although numerous researchers demonstrated the significant difference in performance between the various beam-to-column connection types, most of the previous studies in the area of infilled steel frames focused on the behaviour of frames with welded connections. Therefore, there is a need for conducting studies on infilled steel frames with other common connection types (extended endplate with and without rib stiffeners, flush endplate and shear connections). In this paper, firstly, a two-dimensional finite-element model simulating the cyclic response of infilled steel frames was presented. The infill-frame interaction, as well as the interactions between connections' components, were properly modelled. Using the previously-validated model, a parametric study on infilled steel frames with five different beam-to-column connection types, under cyclic loading, was carried out. Several parameters, including infill material, fracture energy of masonry and infill thickness, were investigated. The results showed that the infilled frames with welded connections had the highest initial stiffness and load-carrying capacity. However, the infilled frames with extended endplate connections (without rib stiffeners) showed the greatest energy dissipation capacity and about 96% of the load-carrying capacity of frames with welded connections which indicates that this type of connection could have the best performance among the studied connection types. Finally, a simplified analytical model for estimating the stiffness and strength of infilled steel frames (with different beam-to-column connection types) subjected to lateral cyclic loading, was suggested.

Keywords: steel framed buildings; masonry infill; finite element modelling; end-plate connections; header plate connections; welded connections; hysteretic curve; cyclic load

1. Introduction

In urban areas, steel and reinforced concrete (RC) structures are commonly infilled with masonry panels. Such structures, which are referred to as infilled frames, have high lateral stiffness, strength and energy dissipation capacity. Although these masonry walls interact with the bounding frames under earthquake loading and generally modify the dynamic response of structures, they are still treated, in some standards, as non-structural elements during the structural design process, leading to inaccurate results.

Since 1960s, many experimental and finite element studies have been carried out to explore the performance of infilled frames. However, most of these researches were done into the vulnerability of infilled RC structures. On the other hand, a relatively small number of studies were performed on infilled steel frames. For example, Dawe *et al*. (1989) experimentally explored the dynamic behaviour of masonry-infilled steel frames and then made a comparison of the experimental results with those of analytical models. Also, Tasnimi and Mohebkhah (2011) reported an experimental programme investigating the dynamic response of steel frames with masonry infill. In another study, Tong *et al*. (2005) performed tests to examine the cyclic behaviour of steel frames infilled with RC walls.

Moreover, Teeuwen *et al*. (2010) experimentally and numerically investigated the behaviour of steel frames with precast concrete infill walls, taking window opening geometry into consideration. To explore the influence of masonry infill on the cyclic behaviour of special concentrically braced frames, Jazany *et al*. (2013) undertook a study combining both the experimental and analytical sides. The study's results proved that the masonry infill existence may enhance the horizontal rigidity and ultimate load of steel frames. In another study, the effect of masonry infill type on infilled steel frames was experimentally investigated by performing quasi-static cyclic loading tests (Markulak *et al*. 2013). Additionally, Baloevic *et al*. (2017), Fang *et al*. (2013), Flanagan and Bennett (1999), Hariri-Ardebili *et al*. (2014), Hoenderkamp *et al*. (2015), Liu and Soon (2012) and Liu and Manesh (2013) carried out tests on steel frames infilled with different infill materials and under different loading, geometrical and structural conditions.

All the above-mentioned experimental studies conducted memorable works on infilled steel frames and demonstrated that the existence of masonry walls has a significant impact on the ultimate load and dissipative

*Corresponding author, Former M.Sc. Student,
E-mail: eladly@ymail.com
[a] Professor
[b] Senior Lecturer
[c] Professor

ISSN: 1229-9367 (Print), 1598-6233 (Online)

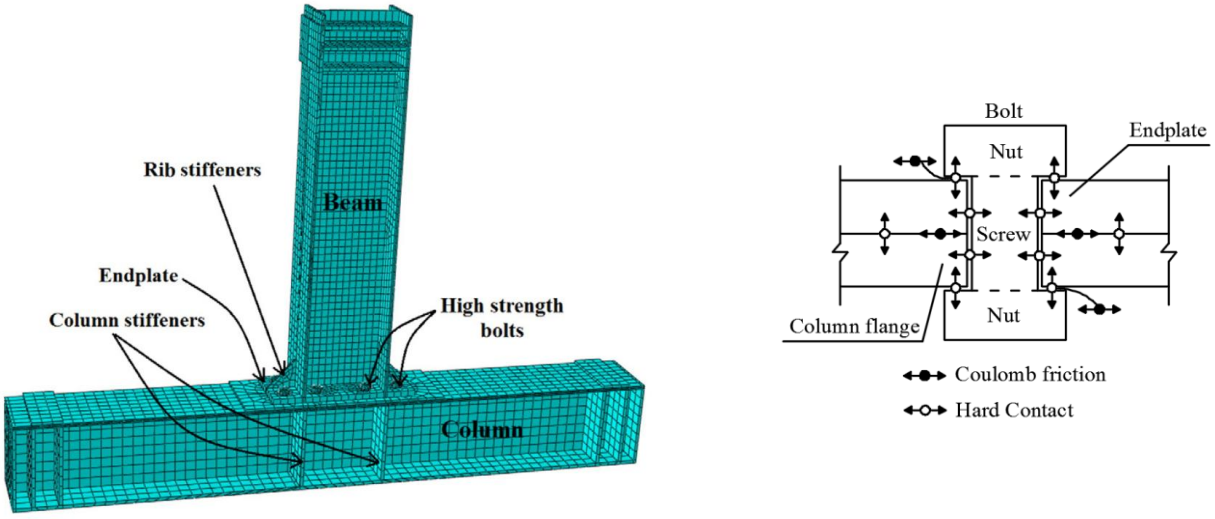

Fig. 1 Interactions between a typical endplate connection's components (Eladly 2017)

energy, as well as the overall behaviour of steel frames under lateral loading.

Moreover, there are some reports for the numerical and analytical simulation of infilled steel frames (Dawe *et al.* 2001a, b, Moghadam *et al.* 2006, Puglisi *et al.* 2009a, b, Asteris *et al.* 2013, Chen and Liu 2016, Quayyum *et al.* 2013, Radnić *et al.* 2013, Radić *et al.* 2016, Yekrangnia and Mohammadi 2017, Eladly 2017). For instance, Dawe *et al.* (2001a) constructed a FE method for modelling the masonry infilled frames. Then, they used it to research the behaviour of masonry-infilled steel frames, considering various parameters (Dawe *et al.* 2001b). Radnić *et al.* (2013) analysed Statically and dynamically the performance of planar steel frames with infill walls, while Asteris *et al.* (2013) presented a comprehensive literature survey of the different micro-models developed to simulate the infilled frames' behaviour. In other studies, two different analytical models of masonry-infilled steel frames were developed and verified by Hariri-Ardebili *et al.* (2014) and Radić *et al.* (2016). Finally, Chen and Liu (2016) and Eladly (2017) carried out research on the effects of gravity loads on the behaviour of steel frames bounding masonry panels.

Although many researchers (Shi *et al.* 2008, Díaz *et al.* 2011, Wang *et al.* 2013, Feizi *et al.* 2015, Ghassemieh *et al.* 2015, El-Khoriby *et al.* 2017, Bayat and Zahrai 2017) confirmed that there is a great difference in performance between the various beam-to-column connection types, almost all of the aforesaid experimental and numerical studies on infilled steel frames investigated the behaviour of frames with welded connections. Thus, there is a necessity to understand the response of infilled steel frames, with other common connection types (extended endplate, flush endplate and shear connections).

In this paper, a FE model was constructed for the analysis of masonry-infilled steel frames' cyclic performance. The model parts, including type of used elements; cyclic constitutive models of steel and infill; contact between beam-to-column connection components as well as between the masonry wall and the bounding frame) were described. Material nonlinearity was taken into consideration. After that, the validated model was used to perform a FE parametric study on cyclically loaded masonry-infilled steel frames with five different beam-to-column connection types (fully welded, extended endplate with rib stiffeners, extended endplate without rib stiffeners, flush endplate and shear connections). The effects of several parameters, including the presence of infill, infill material, fracture energy of masonry and infill thickness, were studied. The strength, rigidity, hysteretic behaviour, dissipative energy and failure modes were compared and researched comprehensively. Furthermore, a simple analytical method, that considers the effect of beam-to-column connection type, was proposed.

2. Finite element analysis

The commercial FEA software ABAQUS was employed to construct a 2D model, representing the dynamic response of infilled steel frames with endplate beam-to-column connections. A typical endplate connection' components and the interactions between them are illustrated in Fig. 1.

The endplate connections' behaviour was simulated based on El-Khoriby *et al.* (2017)'s numerical work, while the modelling of masonry wall and its contact with the surrounding frame was conducted depending on the FE model, for steel frames infilled with masonry panels, presented and verified in Eladly (2017) and in the MSc thesis of the second co-author under the supervision of the

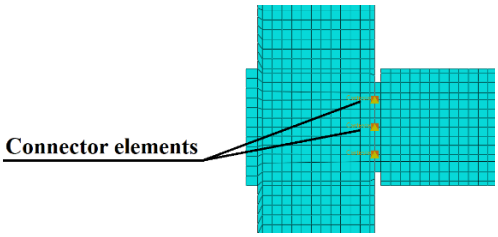

Fig. 2 High-strength bolts represented by connector elements

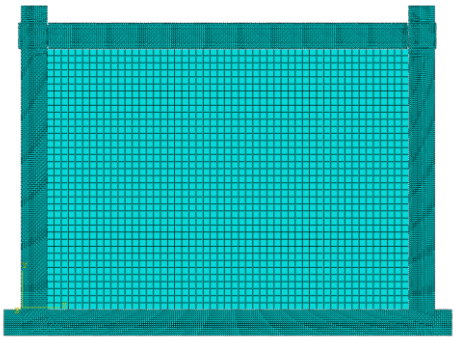

Fig. 3 A 2D FE model of an infilled steel frame

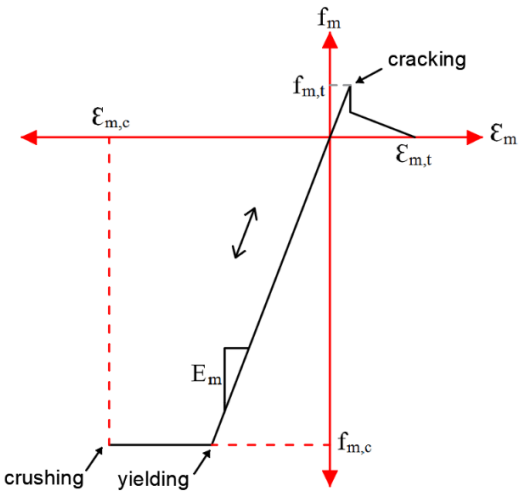

Fig. 4 Adopted constitutive model for masonry

other three co-authors (Eladly 2016). The model is briefly described as follows.CPS4 (a four-node plane stress element) was utilised for the infill panel and steel members. A homogenised macro-model (in which the units, mortar and the unit-mortar interface were represented as one continuum element) was used to mimic the response of the infill wall. This macro-model fits the current study, which explores the overall behaviour of infilled frames, and thus there is no need for performing detailed stress analysis. Many trials have been performed using various mesh sizes (5-50 mm for the steel frame and 25-100 mm for the infill panel) to choose an ideal size of mesh. Fine mesh of elements with approximate size of 23 mm for the steel frame and 82 mm for the infill wall was adopted, as choosing finer mesh does not provide any noticeable improvement in the accuracy of results.

The nodes of endplate and those of column flange were connected by connector elements -rigid plastic CARTESIAN elements- (ABAQUS Analysis User's Manual 2012) in order to simulate the real response of bolts, as shown in Fig. 2. "The connector behaviour was modelled as: (i) rigid up to the slip force limit $P_{slip,i}$; (ii) slip at the bolts up to ± 1 mm (clearance of the bolts to the bolts holes) at constant force $P_{slip,i}$; and (iii) multi-linear plastic behaviour up to the failure load of bolts" (El-Khoriby *et al.* 2017). Additionally, to model the pretension force in bolts,

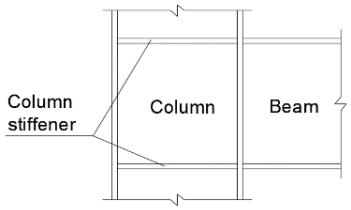

(a) Fully welded (k = 1.00)

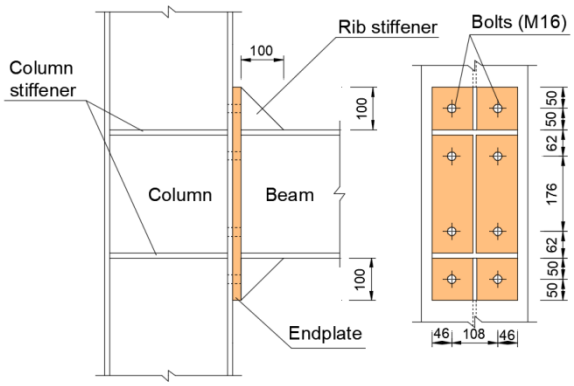

(b) Extended endplate with rib stiffeners (k = 0.86)

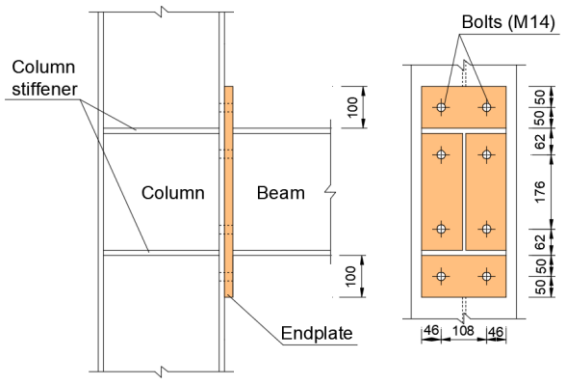

(c) Extended endplate without rib stiffeners (k = 0.72)

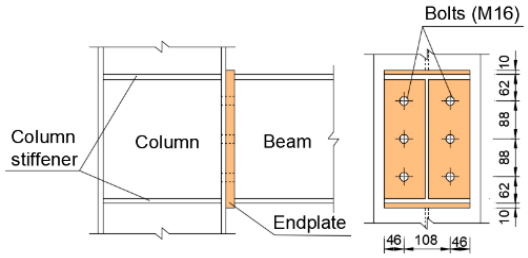

(d) Flush endplate (k = 0.48)

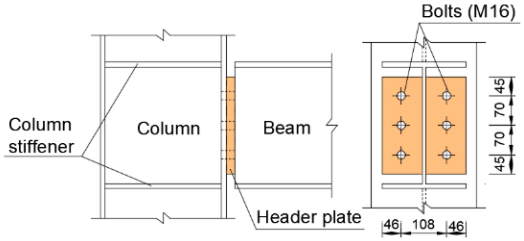

(e) Header plate (k = 0.23)

Fig. 5 Details of the five studied connection types [k is an initial stiffness ratio and can be calculated using Eq. (4)]

"Connector Force" command was utilised.

For the contact between the endplate and column flange, "Hard contact" and "Coulomb friction" were, respectively, used for the normal and tangent interactions (with friction coefficient of 0.44 between steel surfaces, according to Shi *et al*. (2008)'s numerical results). In terms of the frame-infill contact, "Hard contact" was utilised for the normal contact, whilst "frictionless formulation" was used for the tangent interaction. A 2D model of an infilled steel frame with extended endplate connections is shown in Fig. 3.

The Chaboche model (Chaboche 1986, 1989) was employed to represent the steel material in the current study. This model can be represented in ABAQUS as a plastic constitutive model with defining its parameters (σ_0, Q_∞, b, C_i, γ_i), where σ_0 is the yield stress at zero plastic strain; C_i and γ_i are the kinematic hardening parameters; Q_∞ and b are the isotropic hardening parameters. These parameters can be obtained by data fitting (Wang *et al*. 2013, El-Khoriby *et al*. 2017).

Regarding the infill material's modelling, the constitutive model presented by Radnić *et al*. (2012), which is suitable for the 2D macro-modelling of infill panels performed in this paper, was used. Fig. 4 shows the adopted model for masonry infill panel and its parameters, where $f_{m,c}$ is the average of the vertical and horizontal compressive strengths; $f_{m,t}$ is the average of the vertical and horizontal tensile strengths; $\varepsilon_{m,c}$ is the average of the vertical and horizontal crushing compressive strains; $\varepsilon_{m,t}$ is the average of the vertical and horizontal cracking tensile strains; E_m is the elastic modulus. These parameters can be obtained from masonry wallet compression and tension tests, in both vertical and horizontal directions. The Concrete Damaged Plasticity (CDP) model in ABAQUS, which was adopted in previous studies (Giordano *et al*. 2002, Agnihotri *et al*. 2013) to represent the behaviour of masonry structural elements showing good accuracy, was utilised in the current research to model the masonry material. This model provides a general capability for the analysis of quasi-brittle materials (e.g., concrete, masonry infill and rock) under arbitrary loading conditions, including monotonic, uniaxial, multiaxial, cyclic, and/or dynamic loading. To define a material in ABAQUS using the CDP model, it is required to specify the compressive and tensile behaviours; in addition to some parameters, including dilation angle, eccentricity, σ_{b0}/σ_{c0}, K and viscosity parameter (ABAQUS Analysis User's Manual 2012).

Table 1 Summary of the FE models in the parametric study

Model No.	Infill presence	Beam-to-column connection type	Infill material	Fracture energy of infill (J/m^2)	Infill panel thickness (mm)
1	Bare	W	--	--	--
2	Bare	Ext-rib	--	--	--
3	Bare	Ext-no-rib	--	--	--
4	Bare	F	--	--	--
5	Bare	H	--	--	--
6	Infilled	W	WI	143	125
7	Infilled	Ext-rib	WI	143	125
8	Infilled	Ext-no-rib	WI	143	125
9	Infilled	F	WI	143	125
10	Infilled	H	WI	143	125
11	Infilled	W	SI	423	125
12	Infilled	Ext-rib	SI	423	125
13	Infilled	Ext-no-rib	SI	423	125
14	Infilled	F	SI	423	125
15	Infilled	H	SI	423	125
16	Infilled	W	SI	225	125
17	Infilled	Ext-rib	SI	225	125
18	Infilled	Ext-no-rib	SI	225	125
19	Infilled	F	SI	225	125
20	Infilled	H	SI	225	125
21	Infilled	W	WI	143	200
22	Infilled	Ext-rib	WI	143	200
23	Infilled	Ext-no-rib	WI	143	200
24	Infilled	F	WI	143	200
25	Infilled	H	WI	143	200

* The meanings of abbreviations are described in Table 2

Table 2 Abbreviations and symbols in the parametric study

Abbreviation	Meaning
W	Fully welded
Ext-rib	Extended endplate with rib stiffeners
Ext-no-rib	Extended endplate without rib stiffeners
F	Flush endplate
H	Header plate
WI	Weak infill having the same properties of the clay masonry infill used in Markulak *et al*. (2013)'s experimental work (with elastic modulus = 3500 MPa; compressive strength = 1.6 MPa; and tensile strength = 0.22 MPa, based on masonry wallet compression and tension tests)
SI	Strong infill having the same properties of the clay masonry infill used in Yuksel *et al*. (2010)'s experimental work (with elastic modulus = 7000 MPa; compressive strength = 4.14 MPa; and tensile strength = 0.65 MPa, based on masonry wallet compression and tension tests)
FE-XX	Fracture energy of masonry (where XX represents the value of fracture energy in J/m2)
IT-XX	Infill thickness (where XX represents the value of infill thickness in mm)
UL	Lateral load-carrying capacity of frame
K_i	Initial stiffness of frame
E_d	Energy dissipation capacity of frame
DR_{max}	Maximum ductility ratio for frame

3. Verification of the FE model

The suggested FE model proved its ability to accurately represent the dynamic response of steel beam-to-column bolted connections in El-Khoriby *et al*. (2017)'s numerical research. On the other hand, the model's capability to simulate the infilled steel frames' behaviour under cyclic loading was verified in Eladly (2017)'s FE study, using experimental results from four different studies, including Markulak *et al*. (2013), Liu and Manesh (2013), Liu and Soon (2012) and Tasnimi and Mohebkhah (2011). The FE model was capable of mimicking the response of infilled frames, whether the frames were under cyclic or monotonic loading, simulating the evident pinching phenomenon of the force–displacement hysteretic curve with high accuracy (Eladly 2017).

4. Parametric study

There is a clear lack of studies investigating the influence of beam-to-column connection type on the overall behaviour of infilled steel frames. Hence, in the current study, the validated 2D shell model described in Section 2 was used to undertake a numerical parametric study, whose main objectives were: (1) to understand the impact of beam-to-column connection type in addition to other parameters on the dynamic response of infilled steel frames; and (2) to figure out which type of steel beam-to-column connections has the best seismic performance when included into an infilled frame.

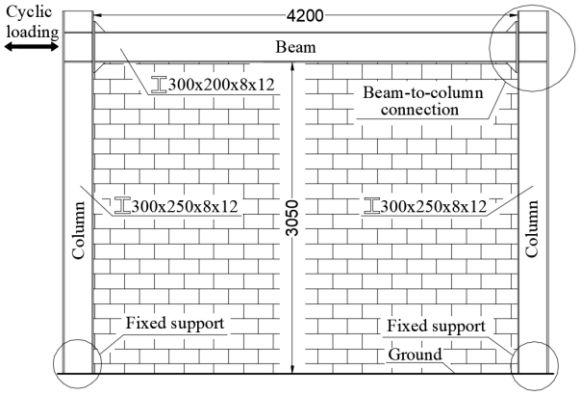

Fig. 6 Steel frame details and dimensions

Table 3 High strength grade 10.9 bolts' material parameters

Elastic modulus (MPa)	Yield strength (MPa)	Ultimate strength (MPa)	Strain at ultimate strength
205000	995	1150	0.137

Table 4 Calibration parameters of Q345B steel (Wang *et al*. 2013)

$\sigma\|0$ (MPa)	Q_∞ (MPa)	B	C_1 (MPa)	γ_1	C_2 (MPa)	γ_2	C_3 (MPa)	γ_3	C_4 (MPa)	γ_4
363.3	21	1.2	7993	175	6773	116	2854	34	1450	29

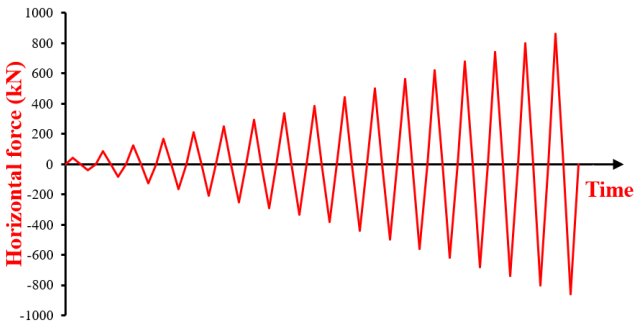

Fig. 7 Loading system

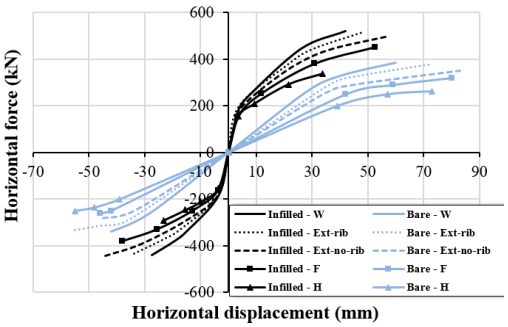

Fig. 8 Hysteretic skeleton curves of bare and infilled frames with different connection types

Thus, the parametric study focused on the cyclic performance of infilled steel frames with five different beam-to-column connection types (fully welded, extended endplate with rib stiffeners, extended endplate without rib stiffeners, flush endplate and header plate connections), whose details are illustrated in Fig. 5. For each connection type, five different cases of masonry infill were considered including: (1) no infill (bare frame); (2) weak infill; (3) strong infill; (4) infill with low fracture energy; and (5) thick infill. These cases were studied for investigating the effects of several parameters (infill material, fracture energy of masonry and infill thickness) which are three of the most important factors influencing the performance of an infill panel. Table 1 summarises the FE models in this parametric study, whilst a list of abbreviations and symbols used in the study is presented in Table 2.

The study was performed on frames with fixed-ended columns, as shown in Fig. 6. H-shaped steel sections were used for the beam and columns. Steel members' dimensions are described in Fig. 6. The thicknesses of endplate, column stiffeners and rip stiffeners were 16 mm, 12 mm and 10 mm, respectively. Standard bolts (Grade 10.9) connected the endplate to the column flange in the four bolted connection types. The diameters of bolts in each connection type are shown in Fig. 5. Pretension forces of 76 kN and

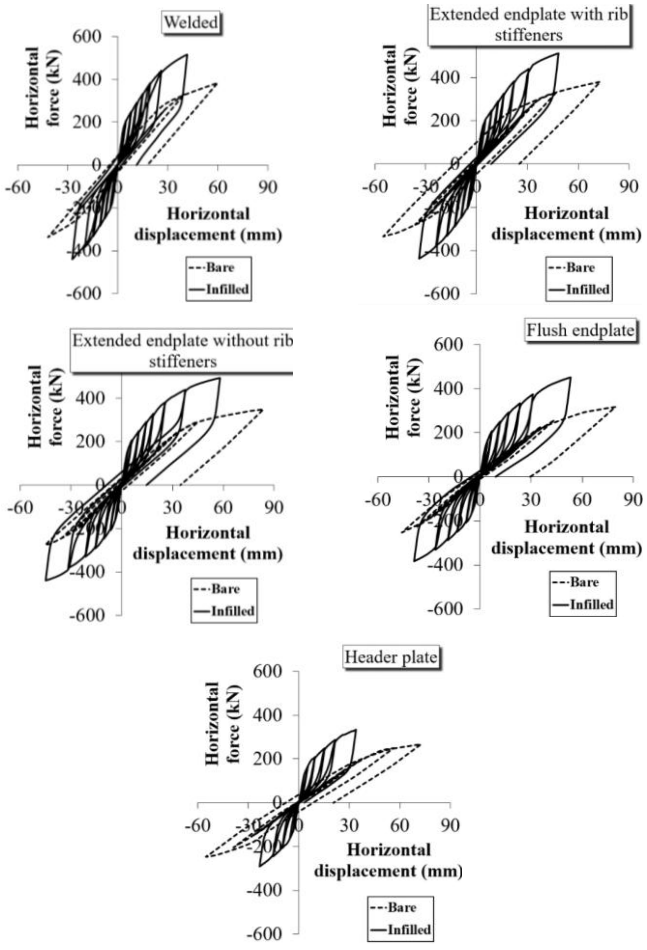

Fig. 9 Hysteretic curves of bare and infilled frames with different connection types

Table 5 Summary of modelling results for bare and infilled steel frames with different connection types

Connection type	Indicator	Frame type	
		Bare	Infilled
W	$UL\ (kN)$	383	515
	$K_i\ (kN/mm)$	9	52
	$E_d\ (kN \cdot mm)$	7659	15019
	$DR_{max}\ (\%)$	1.88	1.31
Ext-rib	$UL\ (kN)$	379	512
	$K_i\ (kN/mm)$	8	51
	$E_d\ (kN \cdot mm)$	13272	17140
	$DR_{max}\ (\%)$	2.28	1.49
Ext-no-rib	$UL\ (kN)$	349	493
	$K_i\ (kN/mm)$	7	50
	$E_d\ (kN \cdot mm)$	13001	23307
	$DR_{max}\ (\%)$	2.59	1.79
F	$UL\ (kN)$	317	450
	$K_i\ (kN/mm)$	6	45
	$E_d\ (kN \cdot mm)$	10391	17936
	$DR_{max}\ (\%)$	2.50	1.64
H	$UL\ (kN)$	266	334
	$K_i\ (kN/mm)$	5	43
	$E_d\ (kN \cdot mm)$	7731	8288
	$DR_{max}\ (\%)$	2.28	1.06

* The meanings of symbols are described in Table 2

99 kN were applied to the M14 and M16 bolts, respectively, in compliance with Eq. (3.1) in Eurocode 3, Part 1.8 (Eurocode 2005). Bolts' material parameters are listed in Table 3, Whereas Q345B steel parameters under cyclic loading are presented in Table 4. In the frames infilled, the length and height of infill walls were, respectively, 4200 mm and 3050 mm, without any special connection, outside adhesion, between these panels and the bounding frames. The properties of the used infill are described in Table 2. As shown in Fig. 6, force-controlled cyclic loading was imposed, at the upper left corner of frame. The loading was imposed according to the loading system illustrated in Fig.7, until the beam-to-column connections regions became fully plastic, causing an unstable plastic mechanism.

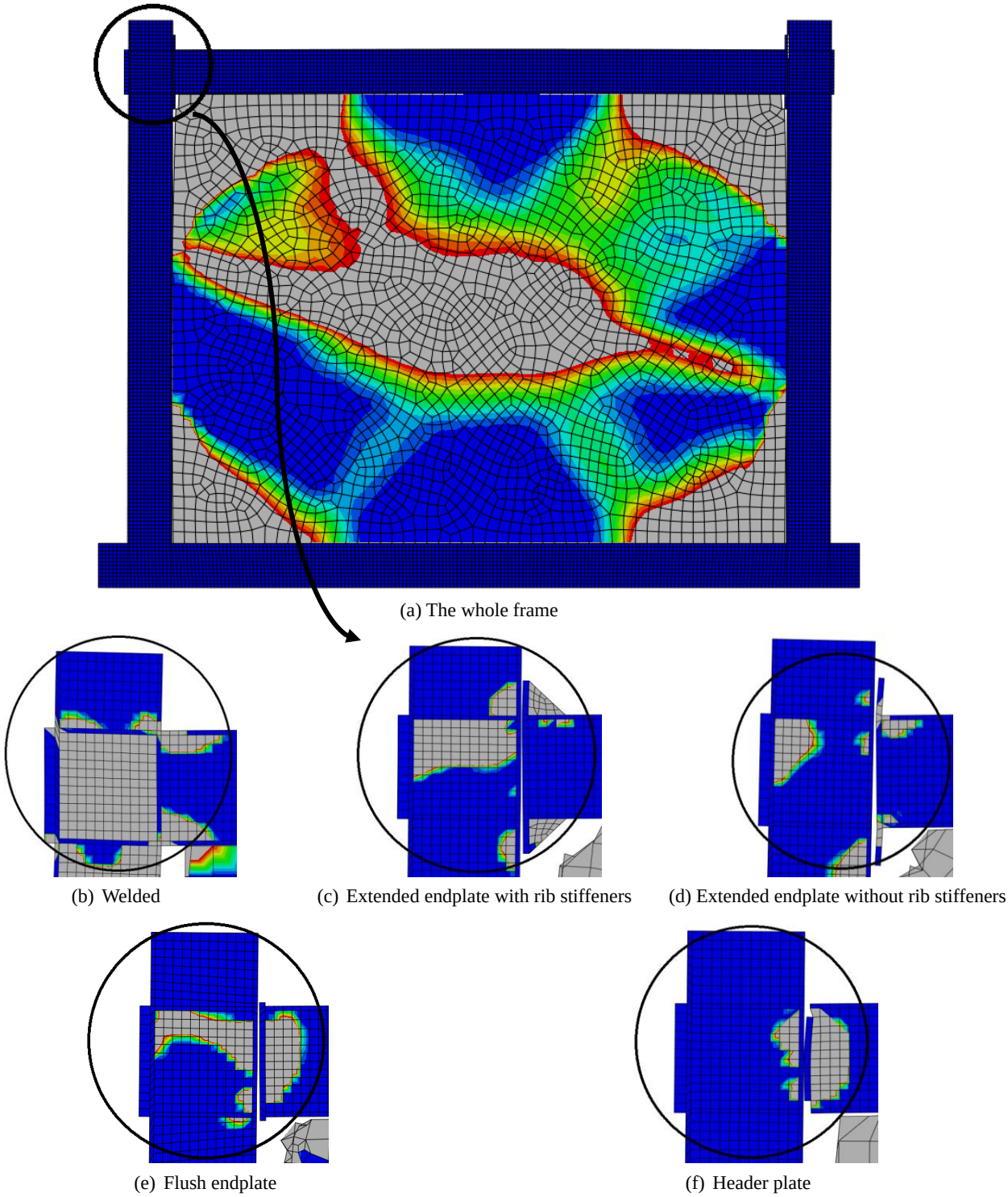

(a) The whole frame

(b) Welded

(c) Extended endplate with rib stiffeners

(d) Extended endplate without rib stiffeners

(e) Flush endplate

(f) Header plate

Fig. 10 (a) Crack patterns in an infill panel bounded by a steel frame with extended endplate connections; and (b-f) equivalent plastic strain in different connection types

5. Results and discussion

5.1 Effect of the presence of infill

Figs. 8, 9 and Table 5, respectively, compare the hysteretic skeleton curves, the hysteretic curves and the performance of bare and infilled steel frames with five different connection types. Three indicators were considered, including load-carrying capacity, initial stiffness and energy dissipation capacity, where the load-carrying capacity is defined as the maximum load that could be carried by the frame; and the energy dissipation capacity can be calculated as the area under force-displacement hysteretic skeleton curve. The imposed horizontal force and the corresponding horizontal displacement were calculated for each increment using the "History Output Requests" option in ABAQUS. In the current section, the studied infilled frames are infilled with weak infill (WI) panels, whose material properties are shown in Table 2.

As shown in the table and figures, regardless of the beam-to-column connection type, infilling the steel frames with masonry walls led to significant enhancements of lateral strength, rigidity and dissipative energy; and reduced the ductility. The infilled frame with welded connections had the highest lateral strength and initial stiffness. However, the infilled frame with extended endplate connections (without rib stiffeners) showed the best performance. Its load-carrying and energy dissipation capacities were, respectively, about 96% and 155% of those of frame with welded connections. This indicates that reducing the stiffness of extended endplate connections included into an infilled steel frame to a certain level (by means of using thinner endplate; removing rib stiffeners; using bolts with smaller diameters; etc.) may improve the overall seismic behaviour of the frame.

Fig. 10 shows the crack patterns in an infill panel and the equivalent plastic strain in different connection types, while compressive stress distribution in an infill wall is shown in Fig. 11. It is clear from Fig. 10(a) that the main failure modes were damage to the core and the four corners of the infill wall. In the case of welded connections (Fig. 10(b)), there is evident panel zone deformation in addition to local buckling of beam flanges. As shown in Fig. 10(c), the extended endplate connection suffered from obvious deformation of panel zone, rib stiffeners and beam flange; a gap between the column flange and the endplate. In the cases of the other three bolted connections shown in Fig. 10(d)-(f), deformation of panel zone (slight) and of endplate and beam flange and web (obvious); a clear gap between the column flange and the endplate; all have occurred. In all the four bolted connection types, when the lateral load (imposed on the frame) increases to a certain level, the column flange-endplate gap increases significantly which eventually leads to bolts rupture.

The beam-infill contact length is another indicator that may provide further clarification of the significant impact of the connection type on infilled frames' performance. As

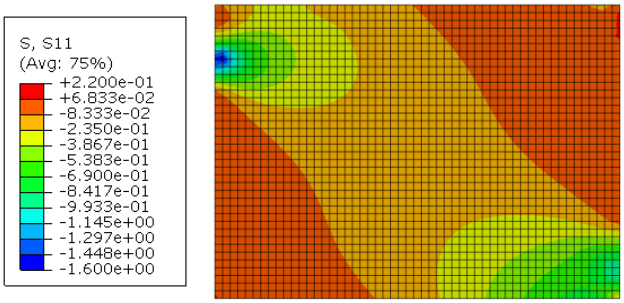

Fig. 11 FE distribution of compressive stress in an infill panel (WI)

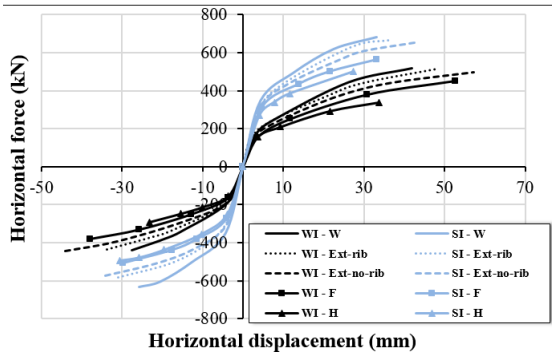

Fig. 12 Hysteretic skeleton curves of infilled frames with different infill materials

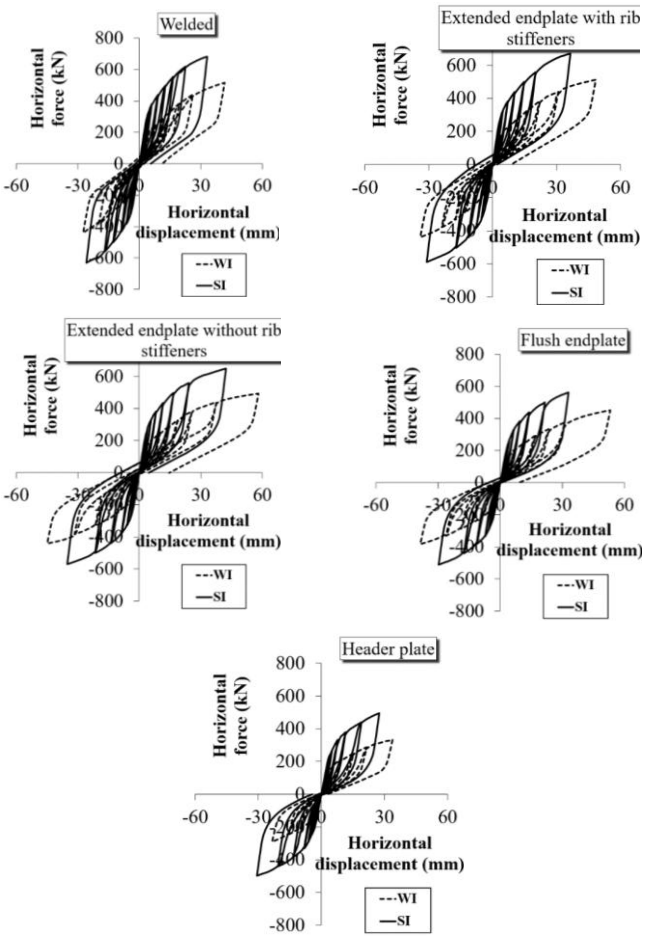

Fig. 13 Hysteretic curves of infilled frames with different infill materials

shown in Table 6, the beam-infill contact length diminishes with the decrease in the connection rigidity. In the frames with relatively low-stiffness connections (e.g. flush endplate and header plate connections), there are deformations of frame members (especially the frame beam) more than in the cases of frames with relatively high-stiffness connections (e.g., extended endplate connections with rib stiffeners), which in turn decreases the contact length between beam and infill panel (Table 6). This decrease in contact length reduces the available loading paths for horizontal force transfer {i.e., decrease the effective width of the equivalent diagonal strut (Smith and Carter 1969) which is substituted for the infill panel in the "equivalent strut" model} and consequently achieves a lower ultimate load.

Table 6 Beam-infill contact length in infilled steel frames with with different connection types (at a lateral load of 250 kN)

Connection type	Beam-infill contact length/ Beam clear span
W	0.31
Ext-rib	0.29
Ext-no-rib	0.27
F	0.22
H	0.20

* The meanings of symbols are described in Table 2

Table 7 Summary of modelling results for infilled frames with different infill materials

Connection type	Indicator	Infill material	
		WI	SI
W	$UL\ (kN)$	515	681
	$K_i\ (kN/mm)$	52	80
	$E_d\ (kN·mm)$	15019	20067
	$DR_{max}\ (\%)$	1.31	1.04
Ext-rib	$UL\ (kN)$	512	670
	$K_i\ (kN/mm)$	51	80
	$E_d\ (kN·mm)$	17140	22533
	$DR_{max}\ (\%)$	1.49	1.14
Ext-no-rib	$UL\ (kN)$	493	650
	$K_i\ (kN/mm)$	50	75
	$E_d\ (kN·mm)$	23307	26589
	$DR_{max}\ (\%)$	1.79	1.33
F	$UL\ (kN)$	450	561
	$K_i\ (kN/mm)$	45	67
	$E_d\ (kN·mm)$	17936	17977
	$DR_{max}\ (\%)$	1.64	1.03
H	$UL\ (kN)$	334	496
	$K_i\ (kN/mm)$	43	65
	$E_d\ (kN·mm)$	8288	15008
	$DR_{max}\ (\%)$	1.06	0.86

* The meanings of symbols are described in Table 2

5.2 Effect of infill material

The infill material's impact on infilled steel frames with different beam-to-column connection types is presented in Table 7. Two different materials (weak infill (WI) and strong infill (SI), whose properties are shown in Table 2) were compared. Comparisons of the hysteretic skeleton curves and hysteretic curves of infilled frames with different infill materials are illustrated in Figs. 12-13, respectively.

From the table and figures, the lateral strength, rigidity and dissipative energy increased (and the ductility decreased) as a result of using stronger infill. These improvements were more obvious in the case of header plate joints than in the other studied joints. For example, using stronger infill led to an improvement of 14% in the energy dissipation capacity of the frame with extended endplate connections (without rib stiffeners). However, in the case of frames with header plate connections, the improvement in the energy dissipation capacity reached 81% as a result of using stronger infill.

It was also noticed that the infilled frames with welded connections showed the highest strength and rigidity (whether the infill is strong or weak); however, the infilled frames with extended endplate connections (without rib stiffeners) had the best energy dissipation capacity.

Moreover, the outcomes showed that the impact of beam-to-column connections on the frames' response was greater in the weak-infilled frames than in the strong-infilled frames. An instance of that is the energy dissipation capacity of strong- and weak-infilled frames with welded connections, which was, respectively, 134% and 181% of that of the same frames but with header plate connections. The reason for this is that in the strong-infilled frames, the relative frame-to-infill stiffness is higher than in the weak-infilled frames. As a result, the ratio of stiffness of beam-to-column connections to that of total infilled frame is less in the latter frames than in the former frames. Thus, the impact of the beam-to-column connection type decreases with the increase in the stiffness of the infill panel.

It was also concluded that the performance of a frame with header plate connections infilled with strong infill was

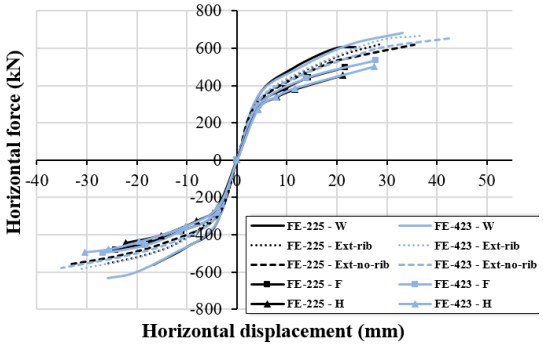

Fig. 14 Hysteretic skeleton curves of steel frames with infill walls with different fracture energy

Table 8 Summary of modelling results for steel frames with infill walls with different fracture energy

Connection type	Indicator	Fracture energy of infill	
		FE-225	FE-423
W	UL (kN)	598	681
	K_i (kN/mm)	80	80
	E_d ($kN·mm$)	11374	20067
	DR_{max} (%)	0.74	1.04
Ext-rib	UL (kN)	627	670
	K_i (kN/mm)	80	80
	E_d ($kN·mm$)	15989	22533
	DR_{max} (%)	0.90	1.14
Ext-no-rib	UL (kN)	620	650
	K_i (kN/mm)	75	75
	E_d ($kN·mm$)	21291	26589
	DR_{max} (%)	1.11	1.33
F	UL (kN)	499	561
	K_i (kN/mm)	67	67
	E_d ($kN·mm$)	11126	17977
	DR_{max} (%)	0.76	1.03
H	UL (kN)	454	496
	K_i (kN/mm)	65	65
	E_d ($kN·mm$)	9505	15008
	DR_{max} (%)	0.70	0.86

* The meanings of symbols are described in Table 2

Table 9 Summary of modelling results for steel frames with infill walls with different thicknesses

Connection type	Indicator	Infill thickness	
		IT-125	IT-200
W	UL (kN)	515	631
	K_i (kN/mm)	52	68
	E_d ($kN·mm$)	15019	19512
	DR_{max} (%)	1.31	1.31
Ext-rib	UL (kN)	512	606
	K_i (kN/mm)	51	63
	E_d ($kN·mm$)	17140	26923
	DR_{max} (%)	1.49	1.52
Ext-no-rib	UL (kN)	493	585
	K_i (kN/mm)	50	60
	E_d ($kN·mm$)	23307	30675
	DR_{max} (%)	1.79	1.80
F	UL (kN)	450	539
	K_i (kN/mm)	45	56
	E_d ($kN·mm$)	17936	23827
	DR_{max} (%)	1.64	1.67
H	UL (kN)	334	499
	K_i (kN/mm)	43	50
	E_d ($kN·mm$)	8288	21435
	DR_{max} (%)	1.06	1.65

* The meanings of symbols are described in Table 2

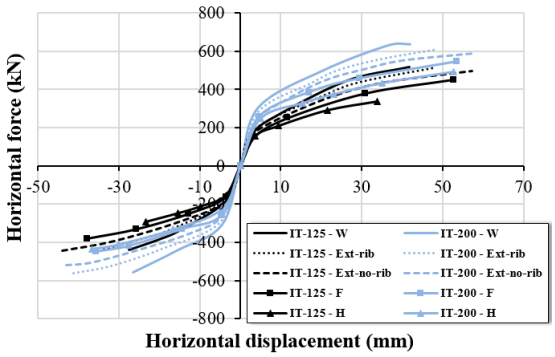

Fig. 15 Hysteretic skeleton curves of steel frames with infill walls with different thicknesses

obviously better than that of a frame with welded connections infilled with weak infill. This means that, a frame combines a strong infill panel and header plate connections can be an economical alternative to one with a weak infill panel and welded connections.

5.3 Effect of fracture energy of masonry

Fracture energy is defined as the energy absorbed to create a unit area of crack surface. It is a fracture mechanics parameter characterising the property of a material to resist cracking and is not affected by the size of structure (Wittmann *et al*. 1990). The fracture energy of masonry can be estimated using the area under the stress versus displacement curve for masonry under uniaxial tension; such response can be obtained by performing tension tests on masonry prisms (Rots 1997). Fig. 14 and Table 8 show the influence of masonry fracture energy on infilled steel frames with different beam-to-column connection types. Two different cases were compared, including infill with fracture energy equal to 225 J/m^2 (FE-225) and infill with fracture energy equal to 423 J/m^2 (FE-423). All frames were infilled with strong infill (SI) panels, whose material properties are shown in Table 2.

From the table and the figure, it can be concluded that, although using infill with higher fracture energy did not increase the initial stiffness, it led to a notable enhancement of the ultimate load, ductility and energy dissipation capacity. This means that an increase in the fracture energy of masonry walls, included into infilled steel frames, may improve the dynamic response of these frames, especially in the cases of welded, flush endplate, or header plate connections.

5.4 Effect of infill panel thickness

Infill panel thickness's influence on steel frames with different beam-to-column connection types is illustrated in

Table 9, whilst Fig. 15 shows the hysteretic skeleton curves of these frames. The influence of two different thicknesses of masonry walls (125 mm and 200 mm) were compared. All frames were infilled with weak infill (WI) panels, whose material properties are shown in Table 2.

From the table and figure, it can be concluded that, for all studied connection types, using thicker infill had a significant effect on the lateral strength, rigidity, ductility and dissipative energy, especially in the cases of header plate connections. This effect is similar to that of using stronger infill (which was previously presented in section 5.2). It is also clear that the frames with extended endplate connections (without rib stiffeners) had the best cyclic response among the studied frames, regardless of infill thickness.

The results also show that the frame with header plate connections infilled with thicker infill not only had better ultimate and energy dissipation capacities than the frame with welded connections infilled with thinner infill, but also showed lower initial stiffness which means that it would have higher time period under real earthquakes. Based on the above, in order to achieve an optimal performance of an infilled steel frame using a cost-effective system, header plate connections in addition to a stiff infill panel may be used instead of welded connections with a weak infill panel.

6. Analytical model

The "equivalent strut" model (Smith and Carter 1969), in which an equivalent pin-jointed diagonal strut is substituted for the infill wall, is one of the most straightforward models for simulating the masonry-infilled frames. Many scholars (Mainstone 1971, Saneinejad and Hobbs 1995, Gambarotta and Lagomarsino 1997a, b, Tasnimi and Mohebkhah 2011) used this concept to construct models representing the infilled frames under lateral loading. Lately, Chen and Liu (2016) and Eladly (2017) followed the same approach to propose analytical methods for estimating the stiffness and lateral ultimate capacity of masonry-infilled steel frames under a combination of lateral and gravity loads. However, almost all of these analytical models for infilled steel frames were developed for frames with welded connections, neglecting the other types of beam-to-column connections. Hence, a modified analytical model is suggested and presented here in the following sections to predict the strength and initial stiffness of infilled steel frames (with different connection types and various material and geometric properties) under lateral cyclic loading.

6.1 Suggested modification factor (M_F)

The results of the parametric study (reported in section 5) demonstrate that the material and geometric properties of masonry infill and the type of beam-to-column connections are primary factors influencing the load-carrying capacity and rigidity of infilled steel frames. The impact of these factors may be taken into consideration by a modification factor to the strength and initial stiffness of infill panels in frames with welded connections; these two indicators can be estimated (for frames with welded connections), simply using the standard equivalent strut model (Smith and Carter 1969, Saneinejad and Hobbs 1995, Tasnimi and Mohebkhah 2011). The proposed modification factor (M_F) can be defined as follows

$$M_F = [1 + f(\lambda L, m)] \times [1 + g(k, \lambda L, m)] \quad (1)$$

where:

- $f(\lambda L, m)$ and $g(k, \lambda L, m)$ are two independent expressions that take into account the influence of relative infill-to-frame stiffness, masonry infill's material properties and beam-to-column connection type by means of three unit-less variables (λL, m and k, respectively).
- λ is a term commonly-used in many former analytical researches on infilled frames (Smith and Carter 1969) and can be expressed as

$$\lambda = \sqrt[4]{\frac{E_m t \sin(2\theta)}{4 E_f I_c H}} \quad (2)$$

  where E_m is the elastic modulus of masonry material; E_f is the elastic modulus of frame material; I_c is the moment of inertia of the frame column; t, L and H are the thickness, length and height of infill; and $\theta = \tan^{-1}(H/L)$. For the frames investigated in this study, the resulted λL values are shown in Table 11.
- m is defined as the fracture energy of masonry infill divided by the compressive capacity of infill per unit length, and can be calculated as

$$m = \frac{G}{f_m' t} \quad (3)$$

  where G is the fracture energy of masonry infill; and f_m' is the infill compressive strength. The m values, for the frames analysed in this paper, are listed in Table 11.
- k is an initial stiffness ratio (for beam-to-column connections), which can be expressed as

$$k = \frac{S_x}{S_w} \quad (4)$$

  where S_x is the initial stiffness of the beam-to-column connection used in the frame, while S_w is the initial stiffness of a fully welded connection connecting the same steel members linked by the former connection. Thus, k is always equal to or less than 1. The initial stiffness of a connection can be calculated through the method presented in section 6.3 in Eurocode 3, Part 1.8 (Eurocode 2005). The k values for the connection types investigated in this research are shown in Fig. 5.

Utilising nonlinear regression analysis on FE results (taking into consideration several equation forms), the expressions of $f(\lambda L, m)$ and $g(k, \lambda L, m)$ were specified as

listed in Table 10. From the table, it is clear that $g(k, \lambda L, m)$ differed based on the connection type and equals 0.00 when the connections are welded (the default case). As the change in infill fracture energy (G) and infill compressive strength ($f_m^{'}$) does not cause any variation in the initial stiffness of infilled frame, $f(\lambda L, m)$ for stiffness is equal to 0.00 as shown in Table 10.

6.2 Comparison with FE results

Using the modified analytical model suggested in section 6.1, the stiffness and strength of masonry-infilled steel frames (with different infill material properties and various beam-to-column connection types) numerically researched in sections 4 and 5 were calculated. The proposed analytical model was able to predict the strength

Table 10 The functions of $f(\lambda L, m)$ and $g(k, \lambda L, m)$ for four connection types

Function	Connection type			
$f(\lambda L, m)$	All connection types	For strength	$-8.95 \times 10^{-7} \times (\lambda L)^{5.98} \times m^{-2.5}$	(5)
		For stiffness	0.00	
$g(k, \lambda L, m)$	Welded	For strength	0.00	
		For stiffness	0.00	
	Extended endplate	For strength	$0.13 \times (\lambda L)^{0.1} \times m^{0.2} \times k^{1.19}$	(6)
		For stiffness	$-0.041 \times (\lambda L)^{-0.72} \times m^{-0.52} \times k^{-2.66}$	(7)
	Flush endplate	For strength	$-3.71 \times 10^{-5} \times (\lambda L)^{3.98} \times m^{-0.22} \times k^{-1.83}$	(8)
		For stiffness	$-5.3 \times 10^{-3} \times (\lambda L)^{1.65} \times m^{-0.12} \times k^{-0.5}$	(9)
	Header plate	For strength	$-1.41 \times (\lambda L)^{-2.6} \times m^{1.07} \times k^{-1.97}$	(10)
		For stiffness	$-0.048 \times (\lambda L)^{-0.025} \times m^{0.02} \times k^{-0.89}$	(11)

Table 11 Comparison of FE and analytical results

Model No.	Beam-to-column connection type	λL	m	k_{FE}^{*} (kN/mm)	P_{FE}^{*} (kN)	k_{Ana}^{*} (kN/mm)	P_{Ana}^{*} (kN)	$\frac{k_{FE}}{k_{Ana}}$	$\frac{P_{FE}}{P_{Ana}}$
6	W	4.68	0.72	52.00	515.00	52.00	504.16	1.00	1.02
7	Ext-rib	4.68	0.72	51.00	512.00	49.78	556.43	1.02	0.92
8	Ext-no-rib	4.68	0.72	50.00	493.00	48.07	484.85	1.04	1.02
9	F	4.68	0.72	45.00	450.00	44.58	428.71	1.01	1.05
10	H	4.68	0.72	43.00	334.00	40.40	430.02	1.06	0.78
11	W	5.56	0.82	80.00	681.00	80.00	652.09	1.00	1.04
12	Ext-rib	5.56	0.82	80.00	670.00	77.33	738.38	1.03	0.91
13	Ext-no-rib	5.56	0.82	75.00	650.00	75.83	677.99	0.99	0.96
14	F	5.56	0.82	67.00	561.00	67.61	565.84	0.99	0.99
15	H	5.56	0.82	65.00	496.00	63.89	469.43	1.02	1.06
16	W	5.56	0.43	80.00	598.00	80.00	658.35	1.00	0.91
17	Ext-rib	5.56	0.43	80.00	627.00	76.72	663.77	1.04	0.94
18	Ext-no-rib	5.56	0.43	75.00	620.00	74.86	589.38	1.00	1.05
19	F	5.56	0.43	67.00	499.00	66.79	546.42	1.00	0.91
20	H	5.56	0.43	65.00	454.00	64.05	502.61	1.01	0.90
21	W	5.26	0.45	68.00	631.00	68.00	544.18	1.00	1.16
22	Ext-rib	5.26	0.45	63.00	606.00	65.68	633.31	0.96	0.96
23	Ext-no-rib	5.26	0.45	60.00	585.00	63.77	577.01	0.94	1.01
24	F	5.26	0.45	56.00	539.00	57.46	477.62	0.97	1.13
25	H	5.26	0.45	50.00	499.00	54.57	439.37	0.92	1.14
							Average	1.00	0.99
							COV (%)	3	9

* k_{FE} and k_{Ana} are the initial stiffness predicted by FE and analytical models, respectively; while P_{FE} and P_{Ana} are, respectively, the load-carrying capacity estimated by FE and analytical models

and stiffness of frames with a high degree of accuracy, as illustrated in Table 11. For all studied frames, a good agreement between the analytical and FE results was realised ($R^2 \geq 0.88$ for strength and ≥ 0.93 stiffness), demonstrating that the suggested analytical model may provide a strong tool for estimating the stiffness and load-carrying capacity of masonry-infilled steel frames with different infill material properties and various connection types, under cyclic lateral loading.

6.3 Application and limitations of the suggested model

The suggested analytical model is applicable to masonry-infilled steel frames subjected to lateral in-plane loading, whether loading is monotonic or cyclic. However, the failure pattern of all infill walls in the frames (investigated in the study) was corner crushing and consequently the suggested equations must be used when this failure mode is the dominant.

To verify (and enhance) the accuracy of the proposed analytical model in calculating the strength and rigidity of infilled steel frames, additional extensive parametric studies on these type of frames (with different beam-to-column connection types and with various geometric and material properties) can be conducted, utilising the simplified finite element model used in this study. The outcomes of these extensive FE studies can be then compared to the analytical model's results to reformulate its equations, if required.

7. Conclusions

To study the cyclic performance of infilled steel frames, a 2D numerical model (which was verified in a previous paper demonstrating its capability of accurately predicting the response of masonry-infilled steel frames to cyclic loading) was utilised. A parametric study on the cyclic behaviour of infilled steel frames with different beam-to-column connection types (fully welded, extended endplate with rib stiffeners, extended endplate without rib stiffeners, flush endplate and header plate connections) was undertaken. Several parameters were investigated including, the presence of infill, infill material, fracture energy of masonry and infill thickness. Based on the study results, the following conclusions can be drawn:

- The cyclic response of infilled steel frames varied considerably depending on the beam-to-column connection type. The horizontal ultimate load of infilled steel frames (WI, IT-125) with welded, flush endplate and header plate connections, was, respectively, 515 kN, 450 kN and 334 kN.
- The infilled frame with welded connections had the highest strength and rigidity. However, the infilled frame (WI, IT-125) with extended endplate connections (without rib stiffeners) showed the best performance, with load-carrying and energy dissipation capacities equal to, respectively, 96% and 155% of those of the same frame but with welded connections. This indicates that reducing the stiffness of extended endplate connections included into an infilled steel frame to a certain level (by means of using thinner endplate; removing rib stiffeners; using bolts with smaller diameters; etc.) may lead to an improvement in the overall frame response to seismic loads.
- Increasing the stiffness of infill panels minimises the impact of beam-to-column connections. For example, the energy dissipation capacity of weak-infilled (WI) and strong-infilled (SI) frames with welded connections was, respectively, 181% and 134% of that of the same frames but with header plate connections.
- Using stiffer (stronger or thicker) infill resulted in significant enhancements of load-carrying and energy dissipation capacities. These enhancements were more obvious in the case of header plate connections than in the other studied connection types.
- The frame with header plate connections infilled with stiffer infill not only had better load-carrying and energy dissipation capacities than the frame with welded connections infilled with weaker infill, but also showed lower initial stiffness which means that it would have higher time period under real earthquakes. Hence, in order to achieve an optimal performance of an infilled steel frame using a cost-effective system, header plate connections in addition to a stiff infill panel may be used instead of welded connections with a weak infill panel.
- A set of equations, for predicting the stiffness and strength of masonry infill panels bounded by steel frames under cyclic loading, was developed. The equations exhibited very good correlation with FE results for cyclically-loaded infilled steel frames with different connection types.

References

ABAQUS (2012), Analysis User's Manual, Version 6.12, Dassault Systèmes; USA.

Agnihotri, P., Singhal, V. and Rai, D.C. (2013), "Effect of in-plane damage on out-of-plane strength of unreinforced masonry walls", *Eng. Struct.*, **57**, 1-11.

Asteris, P.G., Cotsovos, D.M., Chrysostomou, C.Z., Mohebkhah, A. and Al-Chaar, G.K. (2013), "Mathematical micromodeling of infilled frames: State of the art", *Eng. Struct.*, **56**, 1905-1921.

Baloevic, G., Radnic, J., Grgic, N. and Matesan, D. (2017), "Shake-table study of plaster effects on the behavior of masonry-infilled steel frames", *Steel Compos. Struct., Int. J.*, **23**(2), 195-204.

Bayat, M. and Zahrai, S. (2017), "Seismic performance of mid-rise steel frames with semi-rigid connections having different moment capacity", *Steel Compos. Struct., Int. J.*, **25**(1), 1-17.

Chaboche, J.L. (1986), "Time-independent constitutive theories for cyclic plasticity", *Int. J. Plast.*, **2**(2), 149-188.

Chaboche, J.L. (1989), "Constitutive equations for cyclic plasticity and cyclic viscoplasticity", *Int. J. Plast.*, **5**(3), 247-302.

Chen, X. and Liu, Y. (2016), "A finite element study of the effect of vertical loading on the in-plane behavior of concrete masonry infills bounded by steel frames", *Eng. Struct.*, **117**, 118-129.

Dawe, J.L., Schriver, A.B. and Sofocleous, C. (1989), "Masonry infilled steel frames subjected to dynamic load", *Can. J. Civ. Eng.*, **16**(6), 877-885.

Dawe, J.L., Seah, C.K. and Liu, Y. (2001a), "A computer model

for predicting infilled frame behaviour", *Can. J. Civ. Eng.*, **28**(1), 133-148.
Dawe, J.L., Liu, Y. and Seah, C.K. (2001b), "A parametric study of masonry infilled steel frames", *Can. J. Civ. Eng.*, **28**(1), 149-157.
Díaz, C., Victoria, M., Martí, P. and Querin, O.M. (2011), "FE model of beam-to-column extended end-plate joints", *J. Constr. Steel Res.*, **67**(10), 1578-1590.
Eladly, M.M. (2016), "The behavior of masonry infilled steel frames subjected to cyclic loading", M.Sc. Thesis; Tanta University, Tanta, Egypt.
Eladly, M.M. (2017), "Numerical study on masonry-infilled steel frames under vertical and cyclic horizontal loads", *J. Constr. Steel Res.*, **138**, 308-323.
El-Khoriby, S., Sakr, M.A., Khalifa, T.M. and Eladly, M.M. (2017), "Modelling and behaviour of beam-to-column connections under axial force and cyclic bending", *J. Constr. Steel Res.*, **129**, 171-184.
Eurocode (2005), Design of Steel Structures. Part 1.8: Design of joints, European Committee for Standardization; Brussels, Belgium.
Fang, M.J., Wang, J.F. and Li, G.Q. (2013), "Shaking table test of steel frame with ALC external wall panels", *J. Constr. Steel Res.*, **80**, 278-286.
Feizi, M.G., Mojtahedi, A. and Nourani, V. (2015), "Effect of semi-rigid connections in improvement of seismic performance of steel moment-resisting frames", *Steel Compos. Struct., Int. J.*, **19**(2), 467-484.
Flanagan, R.D. and Bennett, R.M. (1999), "Bidirectional Behavior of Structural Clay Tile Infilled Frames", *J. Struct. Eng., ASCE*, **125**(3), 236-244.
Gambarotta, L. and Lagomarsino, S. (1997a), "Damage models for the seismic response of brick masonry shear walls. Part I: the mortar joint model and its applications", *Earthq. Eng. Struct. Dyn.*, **26**(4), 423-439.
Gambarotta, L. and Lagomarsino, S. (1997b), "Damage models for the seismic response of brick masonry shear walls. Part II: the continuum model and its application", *Earthq. Eng. Struct. Dyn.*, **26**(4), 441-462.
Ghassemieh, M., Baei, M., Kari, A., Goudarzi, A. and Laefer, D.F. (2015), "Adopting flexibility of the end-plate connections in steel moment frames", *Steel Compos. Struct., Int. J.*, **18**(5), 1215-1237.
Giordano, A., Mele, E. and De Luca, A. (2002), "Modelling of historical masonry structures: comparison of different approaches through a case study", *Eng. Struct.*, **24**(8), 1057-1069.
Hariri-Ardebili, M.A., Samani, H.R. and Mirtaheri, M. (2014), "Free and Forced Vibration Analysis of an Infilled Steel Frame: Experimental, Numerical, and Analytical Methods", *Shock Vib.*, **2014**, 1-14.
Hoenderkamp, J.C.D., Snijder, H.H. and Hofmeyer, H. (2015), "Racking shear resistance of steel frames with corner connected precast concrete infill panels", *Steel Compos. Struct., Int. J.*, **19**(6), 1403-1419.
Jazany, R.A., Hajirasouliha, I. and Farshchi, H. (2013), "Influence of masonry infill on the seismic performance of concentrically braced frames", *J. Constr. Steel Res.*, **88**, 150-163.
Liu, Y. and Manesh, P. (2013), "Concrete masonry infilled steel frames subjected to combined in-plane lateral and axial loading – An experimental study", *Eng. Struct.*, **52**, 331-339.
Liu, Y. and Soon, S. (2012), "Experimental study of concrete masonry infills bounded by steel frames", *Can. J. Civ. Eng.*, **39**(2), 180-190.
Mainstone, R. (1971), "Summary of paper 7360. On the stiffness and strengths of infilled frames", *Proc. Inst. Civ. Eng.*, **49**(2), 230.
Markulak, D., Radić, I. and Sigmund, V. (2013), "Cyclic testing of single bay steel frames with various types of masonry infill", *Eng. Struct.*, **51**, 267-277.
Moghadam, H.A., Mohammadi, M.G. and Ghaemian, M. (2006), "Experimental and analytical investigation into crack strength determination of infilled steel frames", *J. Constr. Steel Res.*, **62**(12), 1341-1352.
Puglisi, M., Uzcategui, M. and Flórez-López, J. (2009a), "Modeling of masonry of infilled frames, Part I: The plastic concentrator", *Eng. Struct.*, **31**(1), 113-118.
Puglisi, M., Uzcategui, M. and Flórez-López, J. (2009b), "Modeling of masonry of infilled frames, Part II: Cracking and damage", *Eng. Struct.*, **31**(1), 119-124.
Quayyum, S., Alam, M.S. and Rteil, A. (2013), "Seismic behavior of soft storey mid-rise steel frames with randomly distributed masonry infill", *Steel Compos. Struct., Int. J.*, **14**(6), 523-545.
Radić, I., Markulak, D. and Sigmund, V. (2016), "Analytical modelling of masonry-infilled steel frames", *Teh. Vjesn. - Tech. Gaz.*, **23**(1), 115-127.
Radnić, J., Matešan, D., Harapin, A., Smilović, M. and Grgić, N. (2012), *Numerical Model for Static and Dynamic Analysis of Masonry Structures* (*Chapter in Advanced Structured Materials 31 Book, pages 1-33*), Springer Berlin Heidelberg, Heidelberg, Baden-Württemberg, Germany.
Radnić, J., Baloević, G., Matešan, D. and Smilović, M. (2013), "On a numerical model for static and dynamic analysis of in-plane masonry infilled steel frames", *Materwiss. Werksttech.*, **44**(5), 423-430.
Rots, J.G. (1997), *Structural Masonry*: *An Experimental/ Numerical Basis for Practical Design Rules* (*CUR Report 171*), A.A. Balkema Publishers, Rotterdam, South Holland, Netherlands.
Saneinejad, A. and Hobbs, B. (1995), "Inelastic Design of Infilled Frames", *J. Struct. Eng., ASCE*, **121**(4), 634-650.
Shi, G., Shi, Y., Wang, Y. and Bradford, M.A. (2008), "Numerical simulation of steel pretensioned bolted end-plate connections of different types and details", *Eng. Struct.*, **30**(10), 2677-2686.
Smith, B.S. and Carter, C. (1969), "A method of analysis for infilled frames", *Proc. Inst. Civ. Eng.*, **44**(1), 31-48.
Tasnimi, A.A. and Mohebkhah, A. (2011), "Investigation on the behavior of brick-infilled steel frames with openings, experimental and analytical approaches", *Eng. Struct.*, **33**(3), 968-980.
Teeuwen, P.A., Kleinman, C.S., Snijder, H.H. and Hofmeyer, H. (2010), "Experimental and numerical investigations into the composite behaviour of steel frames and precast concrete infill panels with window openings", *Steel Compos. Struct., Int. J.*, **10**(1), 1-21.
Tong, X., Hajjar, J.F., Schultz, A.E. and Shield, C.K. (2005), "Cyclic behavior of steel frame structures with composite reinforced concrete infill walls and partially-restrained connections", *J. Constr. Steel Res.*, **61**(4), 531-552.
Wang, M., Shi, Y., Wang, Y. and Shi, G. (2013), "Numerical study on seismic behaviors of steel frame end-plate connections", *J. Constr. Steel Res.*, **90**, 140-152.
Wittmann, F.H., Mihashi, H. and Nomura, N. (1990), "Size effect on fracture energy of concrete", *Eng. Fract. Mech.*, **35**, 107-115.
Yekrangnia, M. and Mohammadi, M. (2017), "A new strut model for solid masonry infills in steel frames", *Eng. Struct.*, **135**, 222-235.
Yuksel, E., Ozkaynak, H., Buyukozturk, O., Yalcin, C., Dindar, A.A., Surmeli, M. and Tastan, D. (2010), "Performance of alternative CFRP retrofitting schemes used in infilled RC frames", *Constr. Build. Mater.*, **24**(4), 596-609.

CC